The formation and function of focus-like structures of Hfq in long-term nitrogen starved *Escherichia coli*

Josh McQuail, Amy Switzer, Lynn Burchell and Sivaramesh Wigneshweraraj*

MRC Centre for Molecular Bacteriology and Infection, Imperial College London, London, SW7 2AZ, UK

*Corresponding author: E-mail: s.r.wig@imperial.ac.uk; Tel.: +44 207 594 1867.

Abstract

Hfq is an RNA-binding protein that is common to diverse bacterial lineages and has, amongst many, a key role in RNA metabolism. We reveal that Hfq is required by *Escherichia coli* to adapt to nitrogen (N) starvation. By using single molecule tracking photoactivated localisation microscopy imaging of individual Hfq molecules in live *E. coli* cells, we have uncovered an unusual behaviour of Hfq: We demonstrate that Hfq forms a distinct and reversible focus-like structure specifically in long-term N starved *E. coli* cells. We show that foci formation by Hfq is a constituent process of the adaptive response to N starvation and provide evidence which implies that the Hfq foci, analogous to processing (P) bodies of stressed eukaryotic cells, contribute to the management of cellular resources to allow *E. coli* cells to optimally adapt to long-term N starvation stress.

Introduction

Bacteria in their natural environments seldom encounter conditions that support continuous growth. Hence, many bacteria spend the majority of their time in a state of little or no growth, because they are starved of essential nutrients, including carbon, nitrogen and transitional metals. To maximise chances of survival during prolonged periods of nutrient starvation and facilitate optimal growth resumption when nutrients become replenished, bacteria have evolved complex adaptive strategies. Bacteria initially respond to nutrient deficiency by remodelling their transcriptome through the synthesis and degradation of RNA. Nitrogen (N) is an essential element of most macromolecules in a bacterial cell, including proteins, nucleic acids and cell wall components. Thus, unsurprisingly, when *Escherichia coli* cells experience N starvation, they attenuate growth and elicit rapid and large-scale reprogramming of their transcriptome. This results in the synthesis of mRNA encoding proteins associated with transport, and assimilation of nitrogenous compounds into glutamine and glutamate, either catabolically or by reducing the requirement for them in other cellular processes[1-4]. Hence, the adaptive response to N starvation is often dubbed the nitrogen scavenging response.

In addition to mRNA, small regulatory (non-coding) RNA molecules (sRNAs) play an important part regulating the flow of genetic information in response to nutrient starvation in many bacteria[5-9]. sRNAs basepair with target mRNAs leading to enhanced translation or inhibition of translation and/or alteration of mRNA stability[10,11]. In order to form productive interactions with target mRNAs, most sRNAs require a global RNA binding protein (RBP). In many bacteria of diverse lineages, the RBP Hfq plays a central and integral role in sRNA mediated control of gene expression. Emerging results now reveal that, Hfq has diverse functions in bacteria that expands beyond its widely understood role in catalysing sRNA-mRNA basepairing: Hfq has also been demonstrated to play a role in ribosomal RNA

processing and assembly of functional ribosomes[12], tRNA maturation[13] and regulation of RNA degradation[14-17]. Recently, Hfq was shown to contribute to the distribution of sRNA to the poles of *E. coli* cells experiencing (sucrose induced) envelope stress, suggesting a role for Hfq in spatiotemporal regulation of gene expression[18]. Whether Hfq has a role in the adaptive response to N starvation is unknown. Here, we used photoactivated localisation microscopy (PALM) combined with single molecule tracking to study the distribution of individual Hfq molecules in live *E. coli* cells during N starvation. Our results unveil yet another novel behaviour of and role for Hfq, which appears to be an important for maximising the chances of survival during long-term N starvation and allowing optimal growth recovery when N becomes replenished.

Results

The absence of Hfq compromises the ability of *E. coli* to survive N starvation

To determine if Hfq has a role in the adaptive response of *E. coli* to N starvation, we grew a batch culture of wild-type (WT) and Δ*hfq E. coli* in a highly defined minimal growth media with a limiting amount (3 mM) of ammonium chloride (NH_4Cl) as the sole N source[19]. Under these conditions, when NH_4Cl (i.e. N) in the growth medium runs out, the bacteria enter a state of complete N starvation, and subsequent growth attenuation[19]. As shown in Fig. 1a, the initial growth rate (μ) of WT (μ=64.0±0.30 min/generation) and Δ*hfq* (μ=67.3±1.28 min/generation) *E. coli* did not differ greatly. However, as the ammonium chloride levels became depleted (from ~t=3 h; Fig. 1a), the growth rate of the Δ*hfq* (μ=71.3±3.45 min/generation) dropped by ~8% relative to WT bacteria (μ=66.1±0.26 min/generation). Both strains attenuated growth at

the onset of N starvation i.e. the run out of NH_4Cl in the growth medium (~t=4.25 h). We then measured the number of colony forming units (CFU) in the population of WT and Δ*hfq* bacteria as a function of time under N starvation. As shown in Fig. 1b, the proportion of viable cells in the WT population moderately increased over the initial 24 h under N starvation but gradually declined as N starvation ensued beyond 24 h. This initial moderate increase in the portion of viable cells over the initial 24 h was not observed for Δ*hfq* bacteria (Fig. 1b). In contrast, the portion of viable cells in the Δ*hfq* population rapidly decreased as N starvation ensued. For example, after 24 h of N starvation (N-24), only ~27% of the mutant population was viable compared to WT population (Fig. 1b). After 168 h under N starvation (N-168), the majority (~99%) of bacteria in the Δ*hfq* population were nonviable relative to bacteria in the WT population (Fig. 1b). The viability defect of the Δ*hfq* bacteria was partially reversible to that of WT levels when *hfq* was exogenously supplied via a plasmid (Fig. 1b, *inset*). Further, the ability of N-24 Δ*hfq* bacteria to recover growth when inoculated in fresh growth media was delayed by ~107 min compared to that of N-24 WT bacteria although their growth rates (WT ~69.8±1.23 min/generation; Δ*hfq* ~70.3±3.18 min/generation) were comparable once growth had resumed (Supplementary Fig. 1a)

Since Hfq is a major positive regulator of *rpoS* expression[20-23], the RNAP promoter-specificity factor (σ^S), which is responsible for the transcription of diverse stress response associated genes, we considered whether the inability of Δ*hfq* bacteria to adjust their metabolism to cope with N starvation is due to compromised σ^S activity. To investigate this, we calculated, as above, the number of colony forming units (CFU) in the population of Δ*rpoS* bacteria as a function of time under N starvation. The results revealed that, following 24-48 h of N starvation, the Δ*rpoS* bacteria were significantly better at surviving N starvation than Δ*hfq* bacteria (Fig. 1b). For example, at N-24, ~82% of Δ*rpoS* were viable relative to WT bacteria. In contrast, at N-24, only ~27% of the Δ*hfq* bacteria were viable. After 48 h under N starvation,

the Δ*rpoS* bacteria displayed a better ability to survive N starvation than the Δ*hfq* bacteria (Fig. 1b). Further, unlike N-24 Δ*hfq* bacteria, N-24 Δ*rpoS* bacteria did not display a delay in growth recovery when inoculated into fresh growth media (Supplementary Fig. 1b). Overall, we conclude that Hfq contributes to the adaptive response of *E. coli* to N starvation by maximising the chances of survival as N starvation ensues and enabling optimal growth recovery upon repletion of N. Both of these roles of Hfq in the adaptive response to N starvation – at least partly – manifest themselves independently of its role in the regulation of *rpoS*.

Hfq forms a single focus in long-term N starved *E. coli* cells

To better understand the role of Hfq in the adaptive response to N starvation, we used PALM combined with single-molecule tracking to study the intracellular behaviour of individual Hfq molecules in live *E. coli* cells that have been starved of nitrogen for short (~0.5 h; N-) and long (24 h; N-24) periods of time. To do this, we constructed an *E. coli* strain containing photoactivatable mCherry (PA-mCherry) fused C-terminally to Hfq at its normal chromosomal location. Control experiments established that the ability of PA-mCherry-tagged Hfq bacteria to survive long-term N starvation was indistinguishable from that of WT bacteria (Supplementary Fig. 2). We used the apparent diffusion coefficient (*D**) of individual Hfq-PAmCherry molecules, calculated from their mean squared displacement of trajectories, as a metric for the single molecule behaviour of Hfq. During N replete conditions (N+) and at N-, the *D** values of Hfq molecules were largely similar (Fig. 2). However, in bacteria at N-24, we detected a large increase in the proportion of molecules with a lower *D**. Strikingly, this was due to Hfq forming a *single* focus-like feature (~250 nm in diameter), which was present usually, but not exclusively, at the cell pole (Fig. 2). These features, hereafter referred to as the Hfq foci, was seen in ~90% of the cells from N-24 that we analysed. The *D** value of the

majority (~75%) Hfq molecules *within* the Hfq foci was <0.08 (Supplementary Fig. 3). We therefore used a D^* of <0.08 as a threshold to define the relatively immobile population of Hfq molecules within the bacterial cells within the field of view imaged (typically ~50-300 bacterial cells). We then calculated the proportion of Hfq molecules within this immobile population as a percentage of total number of tracked Hfq molecules within the bacterial cells within the same field of view imaged to derive a value ($\%H_{IM}$) to indirectly quantify the efficiency of foci formation by Hfq under different conditions. In other words, cells containing detectable Hfq foci will have an increased $\%H_{IM}$ compared to cells without detectable Hfq foci. According to this criteria, the $\%H_{IM}$ values were ~14, ~16, and ~44 in bacteria at N+, N- and N-24, respectively.

The Hfq foci, once formed, persisted for at least 168 h under N starvation (Supplementary Fig. 4). We did not detect any foci under identical experimental conditions in N-24 bacteria in *E. coli* strains with PAmCherry fused to RNA polymerase, MetJ (the DNA binding transcriptional repressor of genes associated with methionine biosynthesis, which is similar in size to Hfq) or ProQ (a new class of sRNA binding protein in bacteria[24-26] (Supplementary Fig. 5). This result suggested that foci formation is a biological property specific to Hfq. Further, we did not detect any Hfq foci when the bacteria were starved for carbon (C; glucose) for 24 h but when N (NH_4Cl) was still available at sufficient amounts to support growth (Supplementary Fig. 6) or in 24 h old stationary phase cultures grown in standard lysogeny broth (Supplementary Fig. 7). This result suggested that Hfq formation is a phenomenon specific to N starvation. Consistent with this view, we also observed Hfq foci formation at N-24 in cultures grown in media containing 3 mM L-glutamine, D-serine or L-aspartic acid as the sole N source (Supplementary Fig. 8). Overall, we conclude that Hfq forms a single focus in long-term N starved *E. coli* cells.

Hfq foci are not aberrant aggregates of Hfq molecules in long-term N starved *E. coli*

To further characterise the Hfq foci, we determined the intracellular levels of Hfq as a function of time under N starvation. As shown in Fig. 3a, the intracellular levels of Hfq did not increase as N starvation ensued (for up to 168 h), which suggested that the Hfq foci seen in *E. coli* from N-24 are unlikely to be due to accumulation of Hfq as N starvation ensued. To determine whether the foci represent aberrant aggregates of Hfq molecules, we used an *E. coli* strain containing a 3x-FLAG-tag fused C-terminally to Hfq at its normal chromosomal location (kindly provided by Prof Jörg Vogel, University of Würzburg) to obtain the faction of aggregated proteins in bacteria from N+, N- and N-24 (as described in [27]) and attempted to identify Hfq by immunoblotting with anti-FLAG antibodies following separation of the samples on a sodium dodecyl sulphate polyacrylamide gel. As shown in Fig. 3b, we did not detect Hfq in any of the fractions containing aggregated proteins (i.e. in the insoluble fraction), whereas Hfq, as expected, was detectable in whole-cell extracts of bacteria from N+, N- and N-24. This suggests that the Hfq foci are unlikely to be aberrant aggregates of Hfq molecules. We thus considered whether the Hfq foci could be liquid-liquid phase separated biomolecular condensates in long-term N starved *E. coli*. We used hexanediol, which has been previously shown to disrupt liquid-liquid phase separated structures in eukaryotic cells[28], to probe whether Hfq foci formation occurs by liquid-liquid phase separation. As shown in Fig. 3c, the Hfq foci formed in N-24 bacteria rapidly dissipated upon the addition of 10% (v/v) of hexanediol. This suggests that the Hfq foci could resemble liquid-liquid phase separated assemblies in long-term N starved *E. coli*. Finally, Fortas et al[29] previously showed that the unstructured C-terminal region of Hfq has the intrinsic property to self-assemble, albeit into long amyloid-like fibrillar structures, *in vitro*. Further, related studies by Taghbalout et al[30] and Fortas et al[29] showed that Hfq forms irregular clusters in exponentially growing *E. coli* cells in lysogeny broth and that

the C-terminal region of Hfq was required for this clustering behaviour of Hfq, respectively. To investigate whether the C-terminal amino acid residues of Hfq contribute to foci formation, we constructed an *E. coli* strain with PAmCherry tag fused to Hfq at its normal chromosomal location, but which had amino acid residues 73-102 deleted ($Hfq_{\Delta 73\text{-}102}$). As shown in Fig. 3d, foci formation by WT Hfq and $Hfq_{\Delta 73\text{-}102}$ did not markedly differ in bacteria at N-24. Overall, we conclude that the Hfq foci (i) are not aberrant aggregates of Hfq molecules in long-term N starved *E. coli*, (ii) are different to Hfq clusters/aggregates previously seen *in vitro* and *in vivo* and (iii) form independently of the C-terminal amino acid residues 73-102.

Hfq foci formation occurs gradually and independently of *de novo* RNA or protein synthesis in long-term N starved *E. coli*

Since no obvious Hfq foci was detectable in cells at N+ and N- and were only evident at N-24 (Fig. 2), we next investigated the dynamics of Hfq foci formation during the first 24 h of N starvation. As shown in Fig. 4a, no Hfq foci were detected in bacteria that had been N starved for 3 hours (i.e. at N-3). However, in bacteria that have been starved of N for ~6 h (N-6), we began to detect clustering of Hfq resembling Hfq foci and by N-12 discernible Hfq foci were clearly seen (Fig. 4a). It seems that Hfq foci formation is a process that occurs gradually over the course of N starvation in *E. coli*. Since N deficiency induces major adaptive reprograming at the transcriptome and proteome levels, we next investigated whether Hfq foci formation is dependent on cellular transcription and/or translation. To do this, we added 100 μ/ml rifampicin (transcription inhibitor) or 150 μ/ml chloramphenicol (translation inhibitor) to bacteria that had been starved of N for ~1 h (when no Hfq foci are seen) and compared the $\%H_{IM}$ values in antibiotic untreated and treated cells at N-24. The amounts of antibiotics used corresponded to ~5-fold minimum inhibitory concentrations of the antibiotics. As shown in Fig. 4b, neither the

inhibition of transcription nor translation prevented Hfq foci formation (%H_{IM} of ~39 for rifampicin treated cells and %H_{IM} of ~43 for chloramphenicol treated cells compared to %H_{IM} of ~44 of untreated cells). Overall, we conclude that Hfq foci formation is a gradual process in N starved *E. coli,* that occurs independently of *de novo* RNA or protein synthesis.

Hfq foci formation is a reversible and constituent process of the adaptive response to N starvation in *E. coli*

Although Hfq foci formation occurs gradually as N starvation ensues, we next investigated whether Hfq foci formation is a result of the initial adaptive response to N starvation in *E. coli*. We thus considered that any perturbation to the adaptive response to N starvation might affect the efficiency by which the Hfq foci are formed during N starvation. To explore this further, we measured the efficiency of Hfq foci formation in the following mutant *E. coli* backgrounds in which the adaptive response to N starvation was perturbed: Δ*glnG* (devoid of the master transcription regulator NtrC that activates the initial adaptive response to N starvation); Δ*relA* (devoid of the major bacterial (p)ppGpp synthetase that is activated by NtrC in response to N starvation[2]); and Δ*rpoS* (devoid of the major RNAP promoter-specificity factor σ^S, the transcription and accumulation of which is positively affected by *relA* and is responsible for the transcription of diverse stress response associated genes). Hfq foci formation appeared to occur moderately faster in the Δ*glnG* bacteria compared to WT bacteria. At N-24, the %H_{IM} values were ~52 in Δ*glnG* bacteria compared to %H_{IM} of ~44 in WT bacteria (compare Fig. 5a and 5b and Supplementary Fig. 9). In contrast, Hfq foci formation appeared to occur relatively slower in Δ*relA* and Δ*rpoS* bacteria compared to WT bacteria. At N-24, the %H_{IM} values were ~34 and ~33 for Δ*relA* and Δ*rpoS* compared to %H_{IM} of ~44 in WT bacteria (compare Fig. 5a with Fig. 5c and 5d and Supplementary Fig. 9). Thus, it seems that when bacteria are unable to

initiate the adaptive response to N run out (i.e. Δ*glnG* mutant), Hfq foci formation occurs sooner than in WT bacteria. This is presumably so because Δ*glnG* bacteria 'perceive' the effects of N starvation faster in the absence of the mechanisms that allow the adaptive process to N starvation to be gradually initiated. Conversely, when the downstream 'effectors' of *glnG* (i.e. Δ*rpoS* and Δ*relA*) are perturbed, Hfq foci formation occurs at a slower rate than in WT bacteria. This is presumably so because Δ*rpoS* and Δ*relA* bacteria are unable to effectively respond to N starvation as it ensues and effectively execute processes that are required for Hfq foci formation. Overall, it seems that Hfq foci formation is a constituent of the adaptive response to N starvation in *E. coli*.

We next considered that if Hfq foci formation is a constituent of the adaptive response to N starvation, then they should dissipate upon replenishment of N. To explore this, we harvested N starved (thus growth attenuated) bacteria at N-24 and inoculated them into fresh growth media. This, as expected, resulted in the resumption of growth and we detected the dissipation of the Hfq foci just ~1 h after inoculation in the fresh growth media (Fig. 6a). To establish whether the dispersion of the Hfq foci was a direct response to the presence of N or because of resumption of growth, we repeated the experiment and inoculated bacteria from N-24 either into fresh growth media that was devoid of either N or C, which, could not support the resumption of growth. In media devoid of N (but one that contained C), we failed to detect the dissipation of the Hfq foci even after ~3 h after inoculation (Fig. 6b). However, strikingly, the Hfq foci begun to dissipate upon inoculation into media that only contained N but not C (Fig. 6c). Thus, we conclude that the Hfq foci are reversible and that their formation and dissipation are a direct response to the availability of N.

The integrity of RNA binding activity of Hfq is important for foci formation

Hfq assembles into an hexameric ring-like structure with at least three RNA binding surfaces located at the proximal face, rim and distal face of the 'ring'[31]. To investigate whether RNA binding activity of Hfq is required for foci formation, we measured the efficiency of foci formation in bacteria containing representative substitutions at key amino acid residues involved in RNA (either sRNA or mRNA) binding. As shown in Fig. 7a, these were the Q8A and D9A mutations at the proximal face, R16A and R17A mutations at the rim and Y25D and K31A mutations at the distal face of Hfq[32]. Although the amino acid substitutions in Hfq used here do not affect the intracellular levels of Hfq molecules compared to that in WT bacteria[32], all the substitutions have been previously shown to negatively impact Hfq function. Hence, unsurprisingly, bacteria containing the Hfq mutants displayed a compromised ability to adapt to N starvation: As shown in Fig. 7b, bacteria containing the Q8A, D9A, Y25D and K31A Hfq mutants displayed varying degrees of compromised ability to survive long-term (in this case 24 h) N starvation compared to WT bacteria. It seems that the R16A and R17A mutations at the rim of Hfq, are not required for maintaining viability during long-term N starvation in *E. coli* (Fig. 7b). Further, as shown in Fig. 7c, bacteria from N-24 containing the R16A, R17A, Y25D and K31A Hfq mutants displayed varying degrees of increased lag phase (defined here as the time taken to reach an OD_{600} of ~0.15) during growth recovery when N was replenished. Interestingly, foci formation at N-24 was perturbed in the case of all the Hfq mutants: As shown in Fig. 7d, foci formation at N-24 in bacteria containing Q8A, R16A, R17A, Y25D and K31A Hfq mutants were compromised compared to WT bacteria. However, the foci formed at N-24 in bacteria containing the D9A Hfq mutant was much denser than the foci formed by WT Hfq. This is consistent with the fact that the D9A mutation causes Hfq to bind RNA with higher

affinity albeit reduced specificity[32]. We conclude that mutations that compromise the RNA binding activity of Hfq (i) negatively affect the ability of *E. coli* to adapt to N starvation (which manifests itself in reduced viability during N starvation and/or compromised ability to resume growth when N becomes replenished) and (ii) perturb foci formation. Therefore, we further conclude that the integrity of RNA binding activity of Hfq is important for foci formation and this view is corroborated by the D9A Hfq mutant, which has a higher affinity for RNA than the WT protein and forms denser, but likely functionally aberrant, foci.

Hfq foci are involved in managing cellular resources to survive long-term N starvation

The results thus far clearly indicate the Hfq foci formation is an important feature of the adaptive response to N starvation in *E. coli*. Therefore, we considered whether the Hfq foci have a role in managing cellular resources as N starvation ensues. Since the T7 phage can infect and replicate in exponentially growing and stationary phase (i.e. starved) *E. coli* cells equally well[33], we used T7 as a 'biological probe' to evaluate the capability of N starved cellular environment of WT and Δ*hfq* bacteria at N- (when Hfq do not form foci) and N-24 (when Hfq foci form) to support T7 replication. Put simply, we reasoned that since T7 heavily relies on bacterial resources for replication, any perturbations to the management of cellular resources during N starvation could have a negative impact on the efficacy of T7 replication. We compared the time it took for T7 to decrease the density (OD_{600}) of the culture of WT bacteria at N- and N-24 by ~50% (T_{lysis}) following infection. We did this by resuspending bacteria from N- and N-24 in media containing ~3 mM NH_4Cl and T7 phage (NH_4Cl was added to re-activate cellular processes that might be required for T7 infection but might have become repressed upon N starvation). As shown in Fig. 8a, the T_{lysis} of a culture of WT bacteria at N- and N-24 was ~62 min and ~106 min, respectively. The T_{lysis} of Δ*hfq* bacteria infected at N-was delayed

by ~17 min compared to WT bacteria and this resulted in moderate growth of the Δ*hfq* bacterial culture before cell lysis was detectable (Fig. 8a). Strikingly, however, T7 replication was substantially compromised in Δ*hfq* bacteria infected at N-24 (Fig. 8a) and detectable lysis of Δ*hfq* bacteria at N-24 was delayed by ~83min compared to WT bacteria. This delay in lysis of Δ*hfq* bacteria at N-24 was partially reversible to that seen in WT bacteria when *hfq* was exogenously supplied via a plasmid (Fig. 8b). Interestingly, identical experiments with 24 h C starved bacteria (that were conducted in media with excess NH_4Cl), did not produce a difference in T_{lysis} between WT and Δ*hfq* bacteria (Fig. 8c). It thus seems that Hfq has a unique role in managing cellular resources during long term N starvation. Control experiments with a Δ*rpoS* strain confirmed that the compromised ability of T7 to replicate in Δ*hfq* bacteria at N-24 was not due to an indirect effect of the absence of Hfq on *rpoS* (Fig. 8d and Fig. 1b). In other words, it seems that the compromised ability of T7 to replicate in Δ*hfq* bacteria at N-24 is due to a direct consequence of the absence of Hfq. Since a large proportion of the Hfq molecules are present within the foci at N-24, we suggest that the Hfq foci are involved in managing cellular resources to survive long-term N starvation.

Discussion

The adaptive response to N starvation in *E. coli* primarily manifests itself through the management of cellular resources to maximise the chances of cell survival and optimal growth recovery when N becomes available. Although the regulatory aspects of the adaptive response to N starvation is well documented, several details of how this adaptive response is executed are not fully understood. This study has now revealed a role for Hfq, a small and highly abundant hexameric RNA binding protein that is found in many bacteria and plays a critical

role, amongst many others, in RNA metabolism, in the adaptive response to N starvation. The absence of Hfq substantially compromises the ability of *E. coli* to survive long-term N starvation and impacts the ability of long-term N starved bacteria to optimally recover growth when N is replenished. Although we do not yet fully understand how Hfq contributes to the adaptive response to N starvation in detail, strikingly, the results here have uncovered that, as N starvation ensues, Hfq forms a single focus-like structure in long-term N starved *E. coli* cells, which is markedly distinct from clustering of Hfq molecules seen previously in *E. coli*[18,29,30]: Foci formation by Hfq seems to be a constituent process of the adaptive response to N starvation and, in support of this view, the repletion of N to long-term N starved *E. coli* cells causes the dispersion of the Hfq foci. Interestingly, the dispersion of the Hfq foci is a direct result of repletion of N and not due to concomitant the resumption of growth, which suggests that the formation and dissipation of the Hfq foci is a direct consequence to the intracellular availability of N and the cellular response to it. The compromised ability of T7 phage to replicate in long-term N starved Δ*hfq E. coli* (when Hfq foci cannot form) implies that Hfq foci contribute to the management of cellular resources during N starvation (further developed below), which clearly are important for maximising chances of cell survival as N starvation conditions ensues and optimal growth recovery when N becomes available. Since T7 can replicate in long-term C starved Δ*hfq E. coli*, it seems unlikely that Hfq is required for T7 replication *per se* and this result further underscores the view that the formation of Hfq foci is a specific response to long-term N starvation.

The observation that foci formation requires the integrity of the amino acid residues involved in RNA binding in Hfq implies that RNA could be a constituent of the Hfq foci and thus the Hfq foci could be ribonucleoprotein complexes. Unfortunately, attempts to specifically stain RNA (using commercially available RNA specific stains) in N-24 bacteria proved to be unsuccessful, which we suspect is due to extremely poor permeability of the bacteria at N-24.

Although future work in the laboratory will now focused on defining the composition and organisation of the Hfq foci, we propose that, at least conceptually, the Hfq foci resemble liquid-liquid phase separated ribonucleoprotein granules similar to eukaryotic P bodies, which are cytoplasmic ribonucleoprotein complexes comprising of complex networks protein-RNA interactions[34-36]. Since the addition of hexanediol, which has been previously shown to disrupt liquid-liquid phase separated structures in eukaryotic cells[28], also disrupts the Hfq foci, we envisage that the Hfq foci could have an analogues function and properties to eukaryotic P bodies in the adaptive response to N starvation. In fact, like P bodies[37-39], the Hfq foci (i) accumulate gradually upon exposure to stress (in this case as N starvation ensues), (ii) dissipate when the stress is removed (in this case when N is replenished), (iii) have a similar order of magnitude of size (~250 nm) to P bodies (~100-400 nm) and (iv) require RNA binding activity for formation. We thus suggest that the Hfq foci, analogous to P bodies, could be sites of RNA management in N starved bacteria to maximise the chances of cell survival during long-term N starvation and optimal growth recovery when N becomes available. For example, the Hfq foci could consist of a network of RNA binding proteins that selectively protect certain mRNA molecules to enable optimal growth recovery when N becomes replenished and RNA degradation enzymes which degrade unwanted RNA molecules to release N from the nitrogenous RNA molecules to maximise the chances of survival as N starvation conditions ensue. Thus, the absence of Hfq foci could result in the 'mismanagement' of RNA resources under N starvation. Such a scenario would explain the inability of T7 phage, which heavily relies on host bacterial resources, to replicate in N-24 Δ*hfq* bacteria where the Hfq foci cannot form. Indeed, the formation of liquid-liquid phase separated structures akin to P bodies is not unprecedented in bacteria as the RNA degradation enzyme RNaseE of *Caulobacter crescentus* has been previously shown to form multiple liquid-liquid phase separated foci in response to

diverse stresses to manage RNA turnover and disassemble when the stress that lead to their formation becomes alleviated[40].

In summary, Hfq is a widely studied pleiotropic regulator of the RNA metabolism in bacteria and recently has been implicated in the localisation of sRNA at the poles of *E. coli* experiencing sucrose stress[18]. The spatiotemporal regulation of RNA is an emerging area of research in bacteriology and this study has now assigned a new role for Hfq in *E. coli* in the adaptation to and recovery from long-term N starvation that occurs through the formation of focus-like structures of Hfq molecules, which physically and functionally resemble eukaryotic P bodies. Thus, the Hfq foci could represent a mechanism to spatiotemporally manage metabolism in long-term N starved *E. coli*. Importantly, this study has also highlighted the importance of the use of conditions of long-term nutritional adversity and growth attenuated bacteria to unveil novel mechanisms that could underpin spatiotemporal regulation of bacterial processes.

Methods

Bacterial strains and plasmids

All strains used in this study were derived from *Escherichia coli* K-12 and are listed in Supplementary Table 1. The Hfq-PAmCherry and MetJ-PAmCherry strains were constructed

using the λ Red recombination method[41] to create an in-frame fusion encoding a linker sequence and PAmCherry, followed by a kanamycin resistance cassette (amplified from the KF26 strain[42]) to the 3′ end of *hfq* and *metJ*. The ProQ-PAmCherry reporter strain (Δ*proQ*+pACYC-*proQ-PAmCherry*) was constructed by first introducing a deletion of *proQ* in MG1655 using the λ Red recombination method to introduce a kanamycin resistance cassette in place of the *proQ* gene. The pACYC-ProQ-PAmCherry plasmids was made by Gibson assembly and used to express ProQ-PAmCherry under the native promoter of *proQ*[43]. The $Hfq_{\Delta 73\text{-}102}$–PAmCherry strain was made using the λ Red recombination method[41], similar to construction of the Hfq-PAmCherry strain, instead with an in-frame fusion of the linker-PAmCherry sequence replacing amino acids 73-102. Gene deletions were introduced into the Hfq-PAmCherry strain as described previously[19]: Briefly, the knockout alleles was transduced using the P1*vir* bacteriophage with strains from the Keio collection[44] serving as donors. To create point mutant derivatives of Hfq-PAmCherry, PCR based site-directed mutagenesis was performed on pACYC-Hfq using primers listed in Supplementary Table 2[45]. The λ Red recombination method[41] was then used to introduce the point-mutations, along with the linker and PAmCherry tag into *E.coli*.

Bacterial growth conditions

Bacteria were grown in Gutnick minimal medium (33.8 mM KH_2PO_4, 77.5 mM K_2HPO_4, 5.74 mM K_2SO_4, 0.41 mM $MgSO_4$) supplemented with Ho-LE trace elements[46], 0.4% (w/v) glucose as the sole C source and NH_4Cl as the sole N source. Overnight cultures were grown at 37 °C, 180 r.p.m. in Gutnick minimal medium containing 10 mM NH_4Cl. For the N starvation experiments 3 mM NH_4Cl was used (see text for details). For C starvation experiments, bacteria were grown in Gutnick minimal media containing 0.06% (w/v) glucose and 10 mM NH_4Cl. The NH_4Cl concentrations in the growth media were determined using the

Aquaquant ammonium quantification kit (Merck Millipore, UK) as per the manufacturer's instructions. The proportion of viable cells in the bacterial population was determined by measuring colony forming units (CFU)/ml from serial dilutions on lysogeny broth agar plates. Complementation experiments used pBAD24-*hfq*-3xFLAG, or pBAD18 as the empty vector control, in Gutnick minimal media supplemented with 0.2% (w/v) L-arabinose at t=0, for induction of gene expression. To observe Hfq foci dissipation, 25 ml of N-24 culture was centrifuged at 3,200 *g* and resuspend in fresh Gutnick minimal media containing different combinations of 0.4% (w/v) glucose and 3 mM NH_4Cl (see text for details).

Recovery growth assay

Bacterial cultures were grown in Gutnick minimal media under N starvation as described above. At N-24, samples were taken and diluted to an OD_{600} of 0.05 in fresh Gutnick minimal media with 3mM NH4Cl and transferred to a flat-bottom 48-well plate. Cultures were then grown at 37 °C with shaking in a SPECTROstar Nano Microplate Reader (BMG LABTECH) and OD_{600} readings were taken every 10 min.

Photoactivated localization microscopy (PALM) and single molecule tracking (SMT)

For the PALM and SMT experiments, the Hfq-PAmCherry (and derivatives), KF26, MetJ-PAmCherry and ProQ-PAmCherry reporter strains were used. The bacterial cultures were grown as described above and samples were taken at the indicated time points, and imaged and analysed as previously described[42,47]. Briefly, 1 ml of culture was centrifuged, washed and resuspended in a small amount of Gutnick minimal media without any NH_4Cl + 0.4% glucose; samples taken at N+ were resuspended in Gutnick minimal media with 3 mM NH_4Cl + 0.4% glucose. For the C starvation experiments, C- and C-24 samples were resuspended in Gutnick minimal media with 10 mM NH_4Cl but no glucose; C+ samples were resuspended in Gutnick

minimal media with 10 mM NH_4Cl and 0.06% glucose. One µl of the resuspended culture was then placed on a Gutnick minimal media agarose pad (x1 Gutnick minimal media with no NH_4Cl + 0.4% glucose with 1% (w/v) agarose); samples taken at N+ were placed on a pad made with Gutnick minimal media with 3 mM NH_4Cl. For the C starvation experiments, C- and C-24 samples were placed on a pad containing 10 mM NH_4Cl but no glucose; C+ samples were placed on a pad containing 10 mM NH_4Cl and 0.06% glucose. Cells were imaged on a PALM-optimized Nanoimager (Oxford Nanoimaging, www.oxfordni.com) with 15 millisecond exposures, at 66 frames per second over 10,000 frames. Photoactivatable molecules were activated using 405 nanometer (nm) and 561 nm lasers. For SMT, the Nanoimager software was used to localize the molecules by fitting detectable spots of high photon intensity to a Gaussian function. The Nanoimager software SMT function was then used to track individual molecules and draw trajectories of individual molecules over multiple frames, using a maximum step distance between frames of 0.6 micrometer (µm) and a nearest-neighbour exclusion radius of 0.9 µm. The software then calculated the apparent diffusion coefficients (D*) for every trajectory over four steps, based on the mean squared displacement of the molecule.

Immunoblotting

Immunoblotting was conducted in accordance to standard laboratory protocols[48]. The following commercial primary antibodies were used: mouse monoclonal anti-DnaK 4RA2 at 1:10,000 dilution (Enzo, ADI-SPA-880), and anti-FLAG M2 at 1:1,000 dilution (Sigma, F1804). Secondary antibody HRP Goat anti-mouse IgG (BioLegend, 405306) was used at 1:10,000 dilution. ECL Prime Western blotting detection reagent was used (GE Healthcare, RPN2232) to develop the blots, which were analysed on the ChemiDoc MP imaging system and bands quantified using Image Lab software.

Purification of insoluble protein fraction

Insoluble protein fractions were purified exactly as previously described[27]. Briefly, aliquots of bacterial culture (5-20 ml) were cooled on ice and cell pellets harvested by centrifugation at 3,200 *g* for 10 min at 4 °C. To extract the insoluble protein fraction, pellets were resuspended in 40 µl Buffer A (10 mM Potassium phosphate buffer, pH 6.5, 1 mM EDTA, 20% (w/v) sucrose, 1 mg/ml lysozyme) and incubated on ice for 30 min. Cells were then lysed by adding 360 µl of Buffer B (10 mM Potassium phosphate buffer, pH 6.5, 1 mM EDTA) followed by sonication (10 second pulse on, 10 seconds off, 40% amplitude, repeated x6 (2 min total time)) on ice. Intact cells were removed by centrifugation at 2,000 *g* for 15 min at 4 °C, the insoluble fraction pellet was collected by centrifugation at 15,000 *g* for 20 min at 4 °C and kept at -80 °C. Pellets were resuspended in 400 µl of Buffer B and centrifuged at 15,000 *g* for 20 min at 4 °C. The pellet was then resuspended in 320 µl Buffer B and 80 µl of 10% (v/v) NP40 was added. Aggregated proteins were then collected by centrifugation at 15,000 *g* for 30 min at 4 °C. This wash step was repeated once more. The NP40 insoluble pellets were once again washed with 400 µl Buffer B. The final insoluble protein pellet was resuspended in 200 µl of Buffer B and 200 µl LDS loading dye and samples were run on a 12 % (w/v) sodium dodecyl sulphate polyacrylamide gel and analysed by Coomassie stain and immunoblotting, in accordance to standard laboratory protocols [48]. To obtain whole cell extract, bacterial pellets were resuspended in 40 µl of buffer A (with no lysozyme) and 50 µl of 2x lithium dodecyl sulphate loading dye was added before boiling the sample for 5 min and analysis by sodium dodecyl sulphate polyacrylamide gel as above.

T7 phage infection assay

Bacterial cultures were grown in Gutnick minimal media as described above to the indicated time-points (N- and N-24 or C- and C-24). Samples were taken and diluted to OD_{600} of 0.3 in Gutnick minimal media containing ~3 mM NH_4Cl and transferred to a flat-bottom 48-well plate together with T7 phage at a final concentration of $4.2x10^9$ phage/ml. Cultures were then grown at 37 °C with shaking in a SPECTROstar Nano Microplate Reader (BMG LABTECH) and OD_{600} readings were taken every 10 min.

References

1 Switzer, A., Brown, D. R. & Wigneshweraraj, S. New insights into the adaptive transcriptional response to nitrogen starvation in Escherichia coli. *Biochem Soc Trans* **46**, 1721-1728, doi:10.1042/BST20180502 (2018).

2 Brown, D. R., Barton, G., Pan, Z., Buck, M. & Wigneshweraraj, S. Combinatorial stress responses: direct coupling of two major stress responses in Escherichia coli. *Microb Cell* **1**, 315-317, doi:10.15698/mic2014.09.168 (2014).

3 Gyaneshwar, P. *et al.* Sulfur and nitrogen limitation in Escherichia coli K-12: specific homeostatic responses. *J Bacteriol* **187**, 1074-1090, doi:10.1128/JB.187.3.1074-1090.2005 (2005).

4 Zimmer, D. P. *et al.* Nitrogen regulatory protein C-controlled genes of Escherichia coli: scavenging as a defense against nitrogen limitation. *Proc Natl Acad Sci U S A* **97**, 14674-14679, doi:10.1073/pnas.97.26.14674 (2000).

5 Amin, S. V. *et al.* Novel small RNA (sRNA) landscape of the starvation-stress response transcriptome of Salmonella enterica serovar typhimurium. *RNA Biol* **13**, 331-342, doi:10.1080/15476286.2016.1144010 (2016).

6 Holmqvist, E. & Wagner, E. G. H. Impact of bacterial sRNAs in stress responses. *Biochem Soc Trans* **45**, 1203-1212, doi:10.1042/BST20160363 (2017).

7 Kwenda, S. *et al.* Discovery and profiling of small RNAs responsive to stress conditions in the plant pathogen Pectobacterium atrosepticum. *BMC Genomics* **17**, 47, doi:10.1186/s12864-016-2376-0 (2016).

8 Gerrick, E. R. *et al.* Small RNA profiling in Mycobacterium tuberculosis identifies MrsI as necessary for an anticipatory iron sparing response. *Proc Natl Acad Sci U S A* **115**, 6464-6469, doi:10.1073/pnas.1718003115 (2018).

9 Mohd-Padil, H. *et al.* Identification of sRNA mediated responses to nutrient depletion in Burkholderia pseudomallei. *Sci Rep* **7**, 17173, doi:10.1038/s41598-017-17356-4 (2017).

10 Balasubramanian, D. & Vanderpool, C. K. New developments in post-transcriptional regulation of operons by small RNAs. *RNA Biol* **10**, 337-341, doi:10.4161/rna.23696 (2013).

11 Desnoyers, G., Bouchard, M. P. & Masse, E. New insights into small RNA-dependent translational regulation in prokaryotes. *Trends Genet* **29**, 92-98, doi:10.1016/j.tig.2012.10.004 (2013).

12 Andrade, J. M., Dos Santos, R. F., Chelysheva, I., Ignatova, Z. & Arraiano, C. M. The RNA-binding protein Hfq is important for ribosome biogenesis and affects translation fidelity. *EMBO J* **37**, doi:10.15252/embj.201797631 (2018).

13 Lee, T. & Feig, A. L. The RNA binding protein Hfq interacts specifically with tRNAs. *RNA* **14**, 514-523, doi:10.1261/rna.531408 (2008).

14 Andrade, J. M., Pobre, V., Matos, A. M. & Arraiano, C. M. The crucial role of PNPase in the degradation of small RNAs that are not associated with Hfq. *RNA* **18**, 844-855, doi:10.1261/rna.029413.111 (2012).

15 Mohanty, B. K., Maples, V. F. & Kushner, S. R. The Sm-like protein Hfq regulates polyadenylation dependent mRNA decay in Escherichia coli. *Mol Microbiol* **54**, 905-920, doi:10.1111/j.1365-2958.2004.04337.x (2004).

16 Le Derout, J. *et al.* Hfq affects the length and the frequency of short oligo(A) tails at the 3' end of Escherichia coli rpsO mRNAs. *Nucleic Acids Res* **31**, 4017-4023, doi:10.1093/nar/gkg456 (2003).

17 Moll, I., Leitsch, D., Steinhauser, T. & Blasi, U. RNA chaperone activity of the Sm-like Hfq protein. *EMBO Rep* **4**, 284-289, doi:10.1038/sj.embor.embor772 (2003).

18 Kannaiah, S., Livny, J. & Amster-Choder, O. Spatiotemporal Organization of the E. coli Transcriptome: Translation Independence and Engagement in Regulation. *Mol Cell*, doi:10.1016/j.molcel.2019.08.013 (2019).

19 Brown, D. R., Barton, G., Pan, Z., Buck, M. & Wigneshweraraj, S. Nitrogen stress response and stringent response are coupled in Escherichia coli. *Nature communications* **5**, 4115, doi:10.1038/ncomms5115 (2014).

20 Battesti, A., Majdalani, N. & Gottesman, S. The RpoS-mediated general stress response in Escherichia coli. *Annu Rev Microbiol* **65**, 189-213, doi:10.1146/annurev-micro-090110-102946 (2011).

21 Soper, T., Mandin, P., Majdalani, N., Gottesman, S. & Woodson, S. A. Positive regulation by small RNAs and the role of Hfq. *Proc Natl Acad Sci U S A* **107**, 9602-9607, doi:10.1073/pnas.1004435107 (2010).

22 Majdalani, N., Chen, S., Murrow, J., St John, K. & Gottesman, S. Regulation of RpoS by a novel small RNA: the characterization of RprA. *Mol Microbiol* **39**, 1382-1394, doi:10.1111/j.1365-2958.2001.02329.x (2001).

23 Majdalani, N., Cunning, C., Sledjeski, D., Elliott, T. & Gottesman, S. DsrA RNA regulates translation of RpoS message by an anti-antisense mechanism, independent of its action as an antisilencer of transcription. *Proc Natl Acad Sci U S A* **95**, 12462-12467, doi:10.1073/pnas.95.21.12462 (1998).

24 Westermann, A. J. *et al.* The Major RNA-Binding Protein ProQ Impacts Virulence Gene Expression in Salmonella enterica Serovar Typhimurium. *MBio* **10**, doi:10.1128/mBio.02504-18 (2019).

25 Holmqvist, E., Li, L., Bischler, T., Barquist, L. & Vogel, J. Global Maps of ProQ Binding In Vivo Reveal Target Recognition via RNA Structure and Stability Control at mRNA 3' Ends. *Mol Cell* **70**, 971-982 e976, doi:10.1016/j.molcel.2018.04.017 (2018).

26 Smirnov, A. *et al.* Grad-seq guides the discovery of ProQ as a major small RNA-binding protein. *Proc Natl Acad Sci U S A* **113**, 11591-11596, doi:10.1073/pnas.1609981113 (2016).

27 Tomoyasu, T., Mogk, A., Langen, H., Goloubinoff, P. & Bukau, B. Genetic dissection of the roles of chaperones and proteases in protein folding and degradation in the Escherichia coli cytosol. *Mol Microbiol* **40**, 397-413, doi:10.1046/j.1365-2958.2001.02383.x (2001).

28 Alberti, S., Gladfelter, A. & Mittag, T. Considerations and Challenges in Studying Liquid-Liquid Phase Separation and Biomolecular Condensates. *Cell* **176**, 419-434, doi:10.1016/j.cell.2018.12.035 (2019).

29 Fortas, E. *et al.* New insight into the structure and function of Hfq C-terminus. *Biosci Rep* **35**, doi:10.1042/BSR20140128 (2015).

30 Taghbalout, A., Yang, Q. & Arluison, V. The Escherichia coli RNA processing and degradation machinery is compartmentalized within an organized cellular network. *Biochem J* **458**, 11-22, doi:10.1042/BJ20131287 (2014).

31 Vogel, J. & Luisi, B. F. Hfq and its constellation of RNA. *Nat Rev Microbiol* **9**, 578-589, doi:10.1038/nrmicro2615 (2011).

32 Zhang, A., Schu, D. J., Tjaden, B. C., Storz, G. & Gottesman, S. Mutations in interaction surfaces differentially impact E. coli Hfq association with small RNAs and their mRNA targets. *J Mol Biol* **425**, 3678-3697, doi:10.1016/j.jmb.2013.01.006 (2013).

33 Tabib-Salazar, A. *et al.* T7 phage factor required for managing RpoS in Escherichia coli. *Proc Natl Acad Sci U S A* **115**, E5353-E5362, doi:10.1073/pnas.1800429115 (2018).
34 Standart, N. & Weil, D. P-Bodies: Cytosolic Droplets for Coordinated mRNA Storage. *Trends Genet* **34**, 612-626, doi:10.1016/j.tig.2018.05.005 (2018).
35 Luo, Y., Na, Z. & Slavoff, S. A. P-Bodies: Composition, Properties, and Functions. *Biochemistry* **57**, 2424-2431, doi:10.1021/acs.biochem.7b01162 (2018).
36 Hubstenberger, A. *et al.* P-Body Purification Reveals the Condensation of Repressed mRNA Regulons. *Mol Cell* **68**, 144-157 e145, doi:10.1016/j.molcel.2017.09.003 (2017).
37 Shah, K. H., Zhang, B., Ramachandran, V. & Herman, P. K. Processing body and stress granule assembly occur by independent and differentially regulated pathways in Saccharomyces cerevisiae. *Genetics* **193**, 109-123, doi:10.1534/genetics.112.146993 (2013).
38 Teixeira, D., Sheth, U., Valencia-Sanchez, M. A., Brengues, M. & Parker, R. Processing bodies require RNA for assembly and contain nontranslating mRNAs. *RNA* **11**, 371-382, doi:10.1261/rna.7258505 (2005).
39 Grousl, T. *et al.* Robust heat shock induces eIF2alpha-phosphorylation-independent assembly of stress granules containing eIF3 and 40S ribosomal subunits in budding yeast, Saccharomyces cerevisiae. *J Cell Sci* **122**, 2078-2088, doi:10.1242/jcs.045104 (2009).
40 Al-Husini, N., Tomares, D. T., Bitar, O., Childers, W. S. & Schrader, J. M. alpha-Proteobacterial RNA Degradosomes Assemble Liquid-Liquid Phase-Separated RNP Bodies. *Mol Cell* **71**, 1027-1039 e1014, doi:10.1016/j.molcel.2018.08.003 (2018).
41 Datsenko, K. A. & Wanner, B. L. One-step inactivation of chromosomal genes in Escherichia coli K-12 using PCR products. *Proceedings of the National Academy of Sciences of the United States of America* **97**, 6640-6645, doi:10.1073/pnas.120163297 (2000).
42 Stracy, M. *et al.* Live-cell superresolution microscopy reveals the organization of RNA polymerase in the bacterial nucleoid. *Proceedings of the National Academy of Sciences of the United States of America* **112**, E4390-4399, doi:10.1073/pnas.1507592112 (2015).
43 Gibson, D. G. *et al.* Enzymatic assembly of DNA molecules up to several hundred kilobases. *Nature methods* **6**, 343-345, doi:10.1038/nmeth.1318 (2009).
44 Baba, T. *et al.* Construction of Escherichia coli K-12 in-frame, single-gene knockout mutants: the Keio collection. *Mol Syst Biol* **2**, 2006 0008, doi:10.1038/msb4100050 (2006).
45 Kunkel, T. A. Rapid and efficient site-specific mutagenesis without phenotypic selection. *Proceedings of the National Academy of Sciences of the United States of America* **82**, 488-492 (1985).
46 Atlas, R. M. *Handbook of Microbiological Media, Fourth Edition*. (CRC Press, 2010).
47 Endesfelder, U. *et al.* Multiscale spatial organization of RNA polymerase in Escherichia coli. *Biophysical journal* **105**, 172-181, doi:10.1016/j.bpj.2013.05.048 (2013).
48 Sambrook, J., Maniatis, T. & Fritsch, E. F. *Molecular cloning : a laboratory manual*. 2nd edn, (Cold Spring Harbor Laboratory Press, 1989).
49 Sauter, C., Basquin, J. & Suck, D. Sm-like proteins in Eubacteria: the crystal structure of the Hfq protein from Escherichia coli. *Nucleic Acids Res* **31**, 4091-4098 (2003).

50 Guzman, L. M., Belin, D., Carson, M. J. & Beckwith, J. Tight regulation, modulation, and high-level expression by vectors containing the arabinose PBAD promoter. *Journal of bacteriology* **177**, 4121-4130, doi:10.1128/jb.177.14.4121-4130.1995 (1995).

Acknowledgments

This work was supported by Wellcome Trust Investigator Award 100958 to S.W. and a Medical Research Council Ph.D. studentship to J.M.

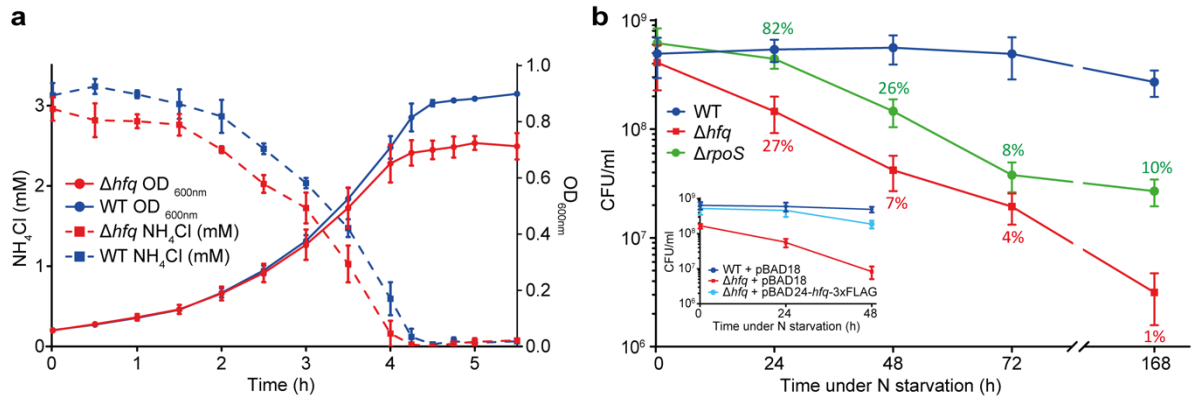

Fig. 1: The absence of Hfq compromises the ability of *E. coli* to survive N starvation.

a Growth and NH_4Cl consumption of WT and Δ*hfq E. coli* grown in N limited conditions. Error bars represent s.d. (n=3). **b** Viability of WT, Δ*hfq* and Δ*rpoS E. coli* during long-term N starvation, measured by counting colony-forming units (CFU). Error bars represent s.d. and each line represents 3 technical replicates of 3 biological replicates. Shown as the insert is the viability of WT and Δ*hfq E. coli* complemented with plasmid-borne *hfq* (pBAD24-*hfq*-3xFLAG) during long-term N starvation, measured by counting CFU.

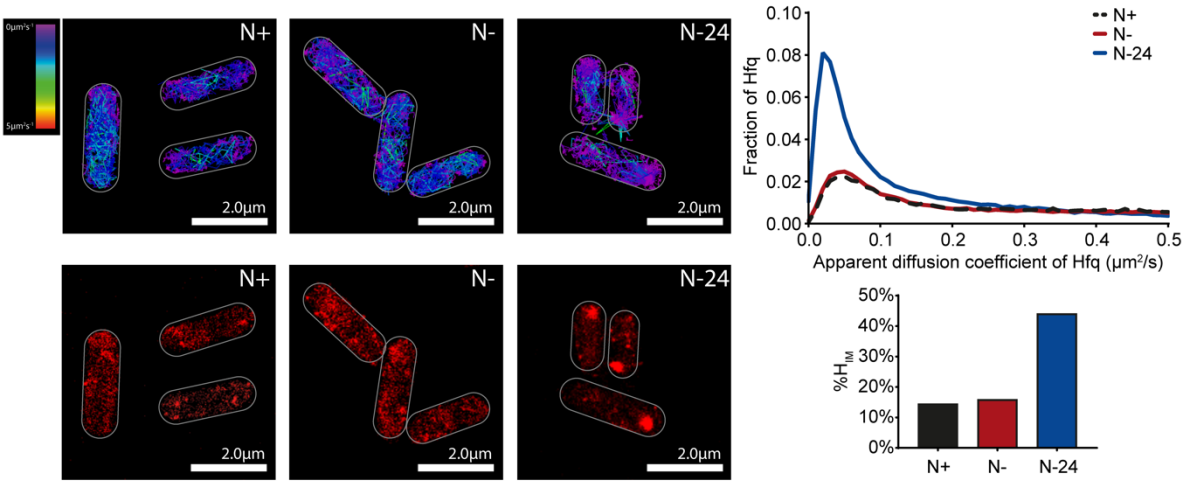

Fig. 2: Hfq forms a single focus in long-term N starved *E. coli* cells.

Representative single molecule tracks and PALM images of Hfq in *E. coli* cells from N+, N- and N-24. The top graph shows the distribution of apparent diffusion co-efficient (*D**) of Hfq molecules and the bottom graph shows $\%H_{IM}$ values.

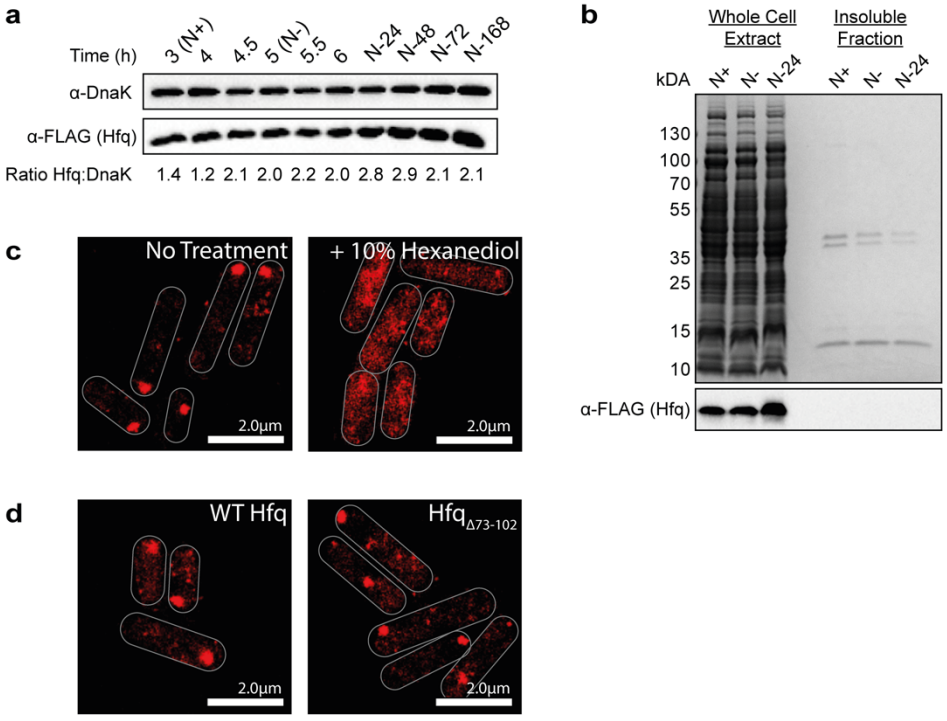

Fig. 3: Hfq foci are not aberrant aggregates of Hfq molecules in long-term N starved *E. coli*

a Representative immunoblot of whole-cell extracts of *E. coli* cells containing Hfq-3xFLAG sampled at 3 h (=N+), 4 h, 4.5 h, 5 h (=N-), 5.5 h and 6 h into growth (as in Fig. 1a), as well as at N-24, N-48, N-72 and N-168. **b** Representative Coomassie stained gel and immunoblot of whole cell extracts and insoluble protein fraction of *E. coli* cells containing Hfq-3xFLAG from N+, N- and N-24. **c** Representative PALM images of Hfq in *E. coli* cells during long-term N starvation with and without treatment with 10% (v/v) hexanediol at N-24. Samples for imaging were taken 1 h after treatment. **d** Representative PALM images of full-length Hfq and C-terminally truncated Hfq ($Hfq_{\Delta 73\text{-}102}$) in *E. coli* cells at N-24.

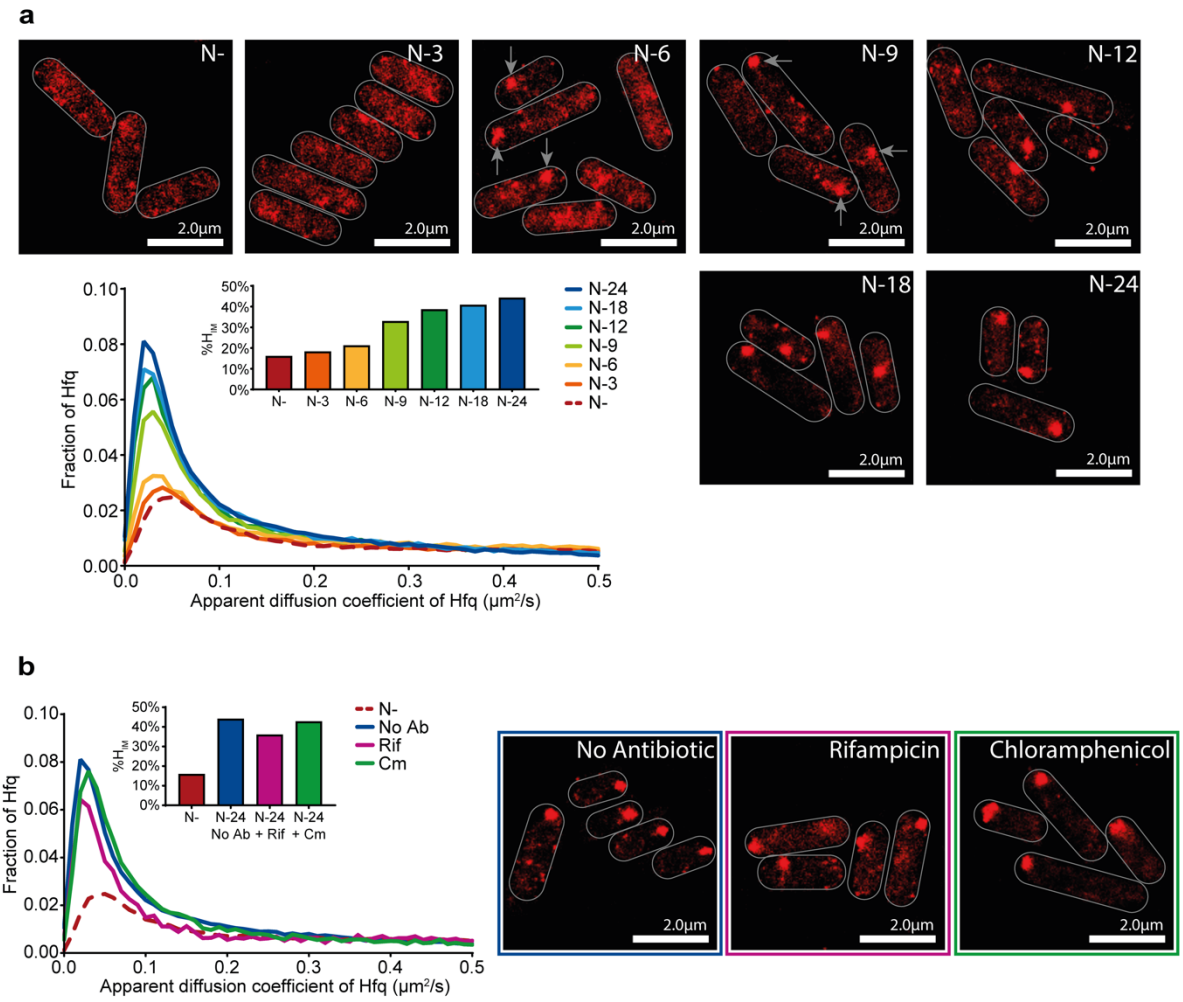

Fig. 4: Hfq foci formation occurs gradually and independently of *de novo* RNA or protein synthesis in long-term N starved *E. coli*.

a Representative PALM images of Hfq in *E. coli* cells as a function of time under N starvation. Images were taken at the indicated time points and the Hfq foci are shown by the arrows. The graph shows the distribution of apparent diffusion co-efficient (*D**) of Hfq molecules at the different sampling time points and the corresponding $\%H_{IM}$ values are shown in the insert graph. **b** Representative PALM images of Hfq in *E. coli* cells that were treated with rifampicin (100 μg/ml) or chloramphenicol (150 μg/ml) 1 h into N starvation (N-1) and imaged at N-24. The PALM image of Hfq in untreated *E. coli* cells is shown as the control. The graph shows the distribution of apparent diffusion co-efficient (*D**) of Hfq molecules and the corresponding $\%H_{IM}$ values are shown in the insert graph.

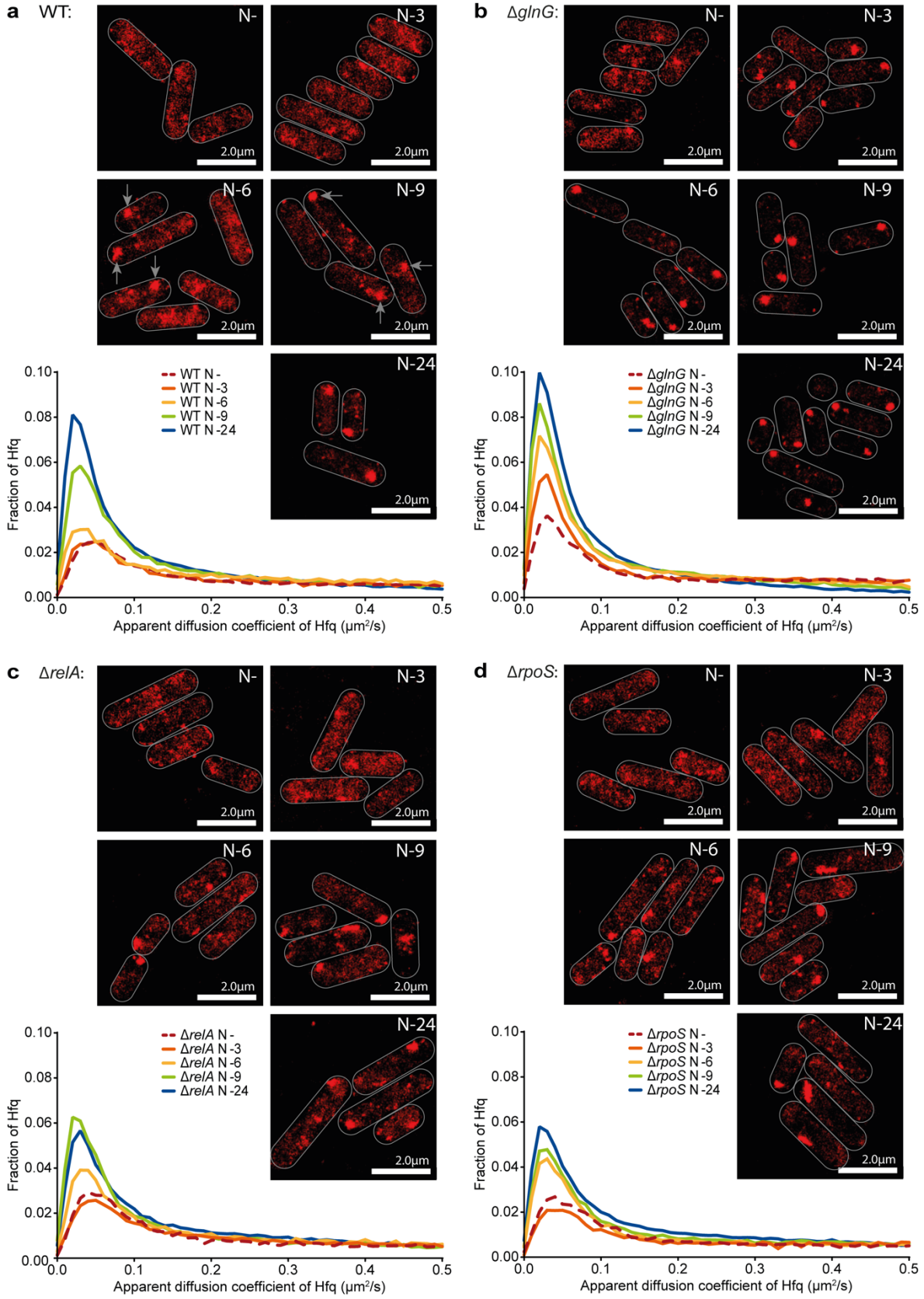

Fig. 5: Hfq foci formation is a constituent process of the adaptive response to long-term N starvation in *E. coli.*

Representative PALM images of Hfq in *E. coli* cells in **a** WT, **b** Δ*glnG*, **c** Δ*relA* and **d** Δ*rpoS* strains, as a function of time under N starvation. The graph shows the distribution of apparent diffusion co-efficient (*D**) of Hfq molecules at the indicated sampling time points. .

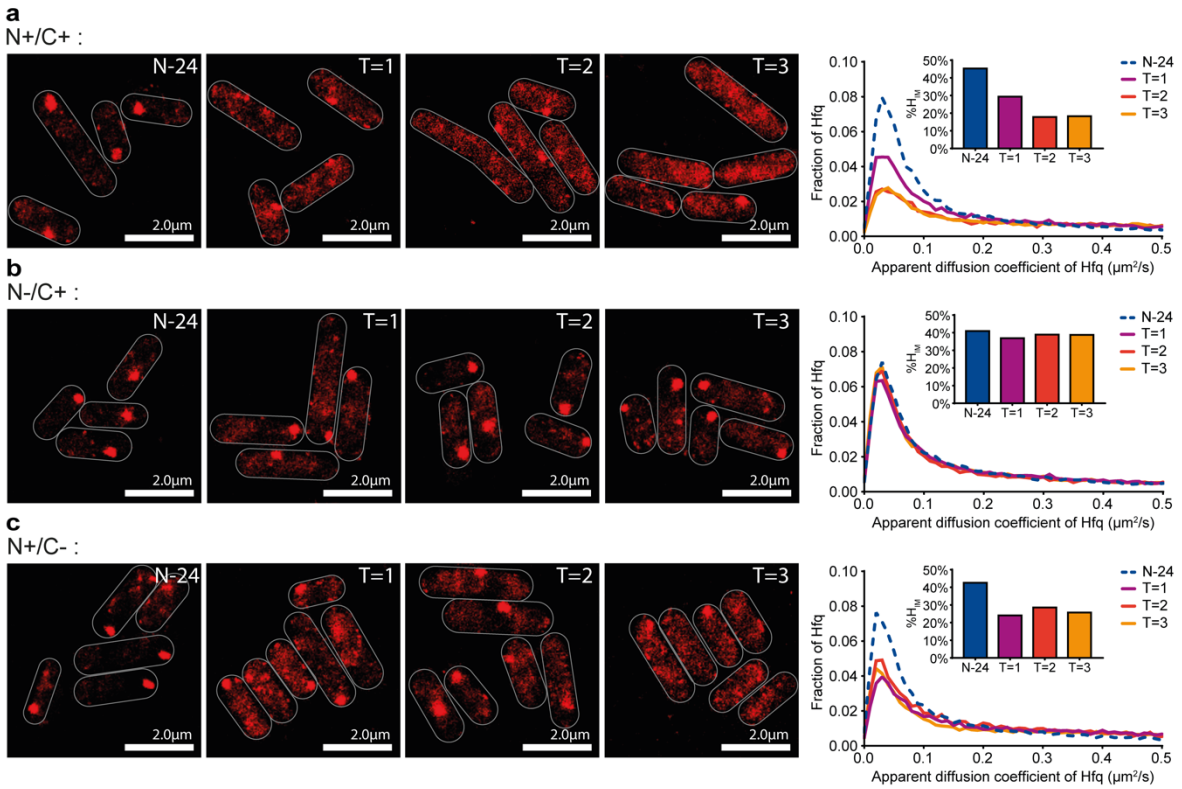

Fig. 6: Hfq foci formation is a reversible process.

Representative PALM images of Hfq from N-24 *E.coli* cells recovered in fresh media with different combinations of N and C (**a** N+/C+, **b** N-/C+, **c** N+/C-). Images taken every hour during recovery growth. The graph shows the distribution of apparent diffusion co-efficient (D^*) of Hfq molecules at the indicated time points and the corresponding $\%H_{IM}$ values are shown in the insert graphs.

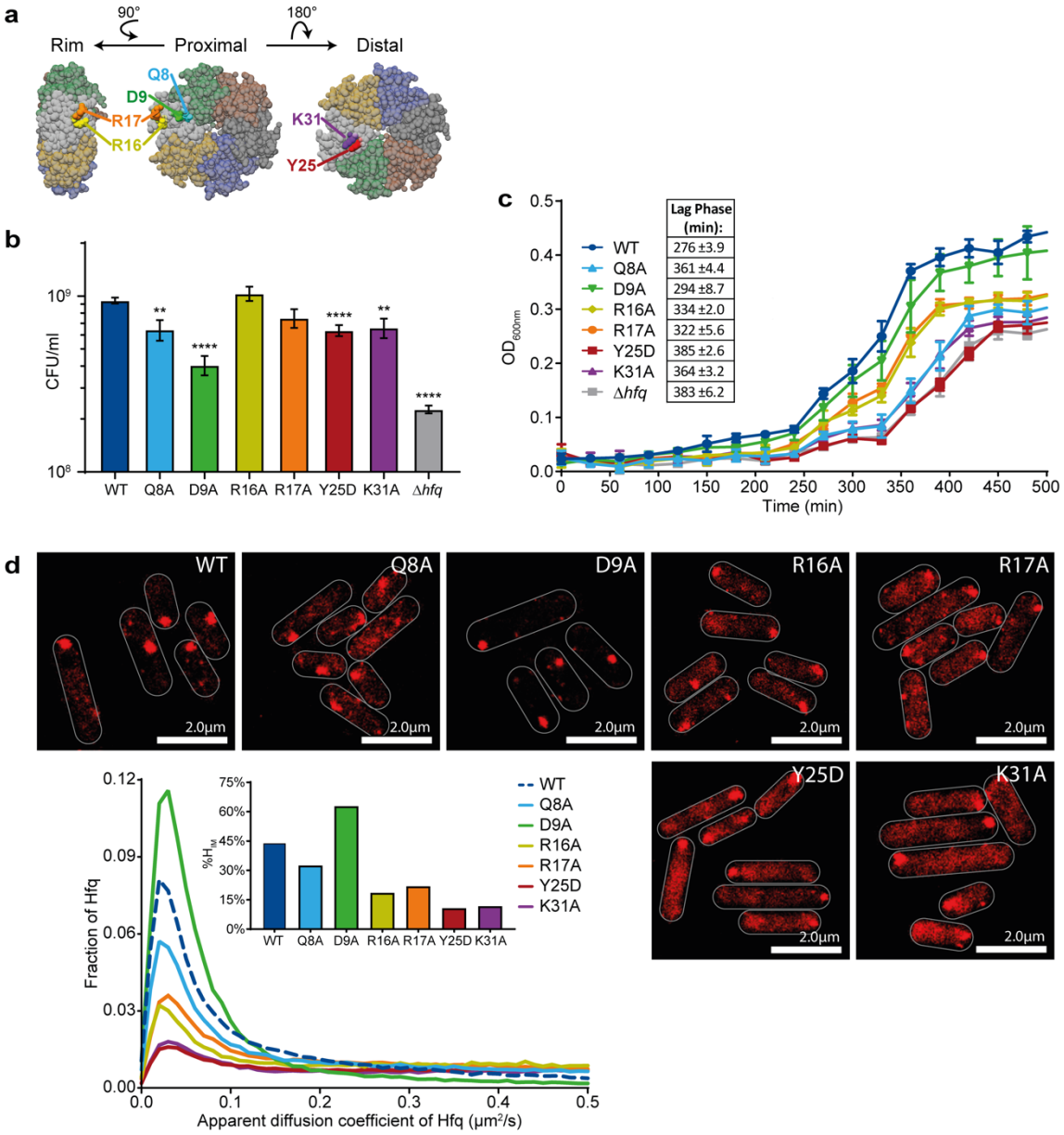

Fig. 7: The integrity of RNA binding activity of Hfq is important for foci formation

a The location of amino acid residues mutated in this study are shown in the crystal structure of Hfq[49]. **b** Viability of WT and mutant *E. coli* cells following 24 h under N starvation measured by CFU counting. Error bars represent s.d. and each bar represents 3 technical replicates of 3 biological replicates. **c** Recovery growth of WT and mutant *E. coli* cells following 24 h under N starvation. Error bars represent s.d. and each line represents 2 technical replicates of 3 biological replicates. The length of lag phase for each strain, defined as the time taken to reach

an OD_{600} of 0.15 is shown in the insert table. **d** Representative PALM images of Hfq in WT and mutant *E. coli* cells sampled at N-24. The graph shows the distribution of apparent diffusion co-efficient (*D**) of Hfq molecules and the corresponding $\%H_{IM}$ values are shown in the insert graph.

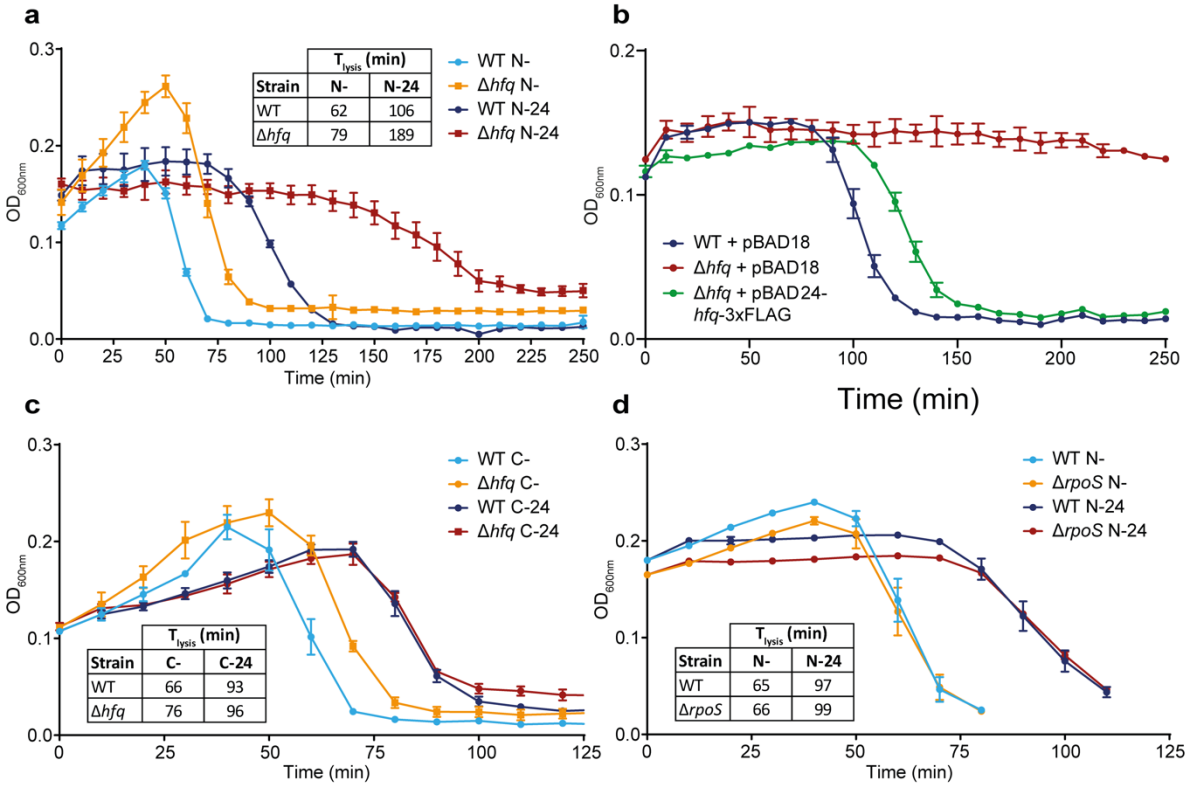

Fig. 8: Hfq foci are involved in managing cellular resources to survive long-term N starvation

a Graph showing the optical density as a function of time of WT and Δ*hfq E. coli* cells from N- and N-24 following infection with T7 phage. Error bars represent s.d. and each line represents 2 technical replicates of 3 biological replicates. The time it takes for the optical density (OD_{600}) of the culture to decrease by ~50% (T_{lysis}) is indicated in the insert table. **b** As in **a**, but the Δ*hfq E. coli* cells were complemented with plasmid-borne *hfq* (pBAD24-*hfq*-3xFLAG). **c** As in **a**, but experiments were conducted under C starvation conditions (see text for details). **d** As in **a**, but experiments were conducted with Δ*rpoS E. coli* cells.

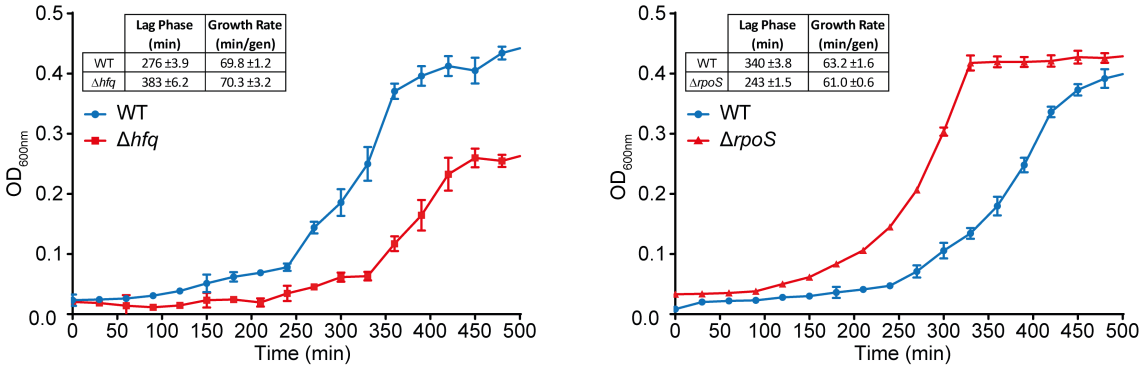

Supplementary Fig. 1: Recovery growth of WT, Δ*hfq* and Δ*rpoS E. coli* cells after long-term N starvation.

Graphs showing the recovery growth dynamics of WT, Δ*hfq* and Δ*rpoS E. coli* cells following 24 h under N starvation. Error bars represent s.d. and each line represents 2 technical replicates of 3 biological replicates. The length of lag phase (defined as the time taken to reach an OD_{600} of 0.15) and growth rate (doubling time) are provided in the insert table.

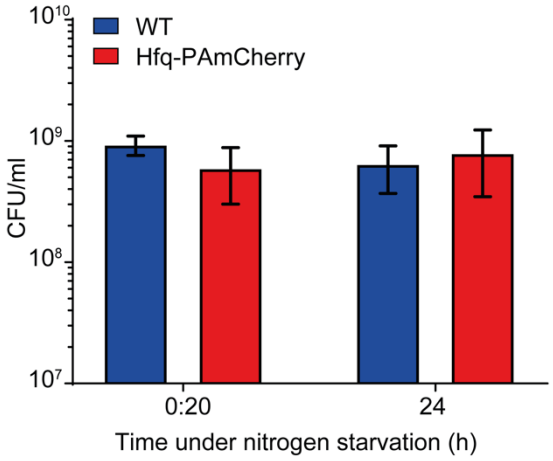

Supplementary Fig. 2: The PAmCherry tag on Hfq does not affect cell viability.

Viability of WT and Hfq-PAmCherry *E. coli* at N- and N-24 measured by CFU. Error bars represent s.d. and each bar represents 3 technical replicates of 3 biological replicates.

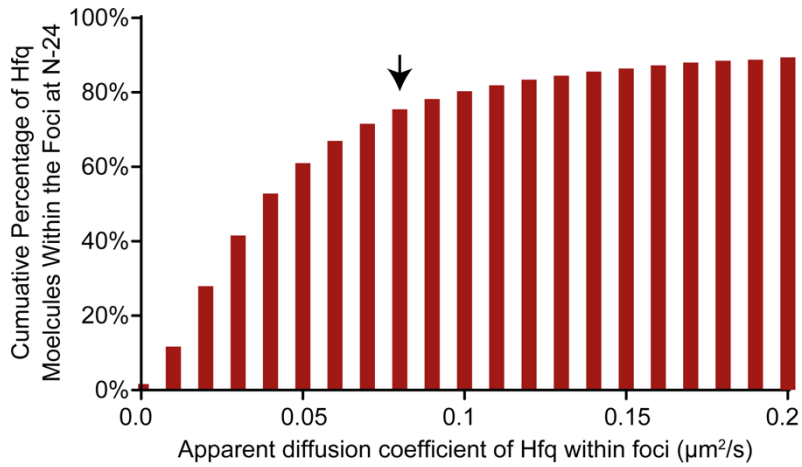

Supplementary Fig. 3: The majority of Hfq molecules in the foci have a *D of <0.08.**

Graph showing the cumulative proportion of Hfq molecules within the foci with increasing values of *D**. Arrow indicates cut-off value used for defining $\%H_{IM}$.

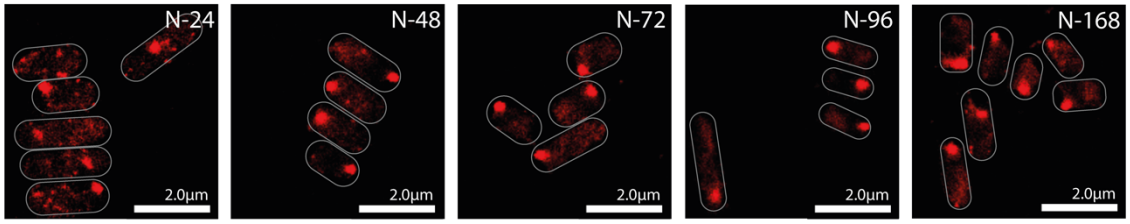

Supplementary Fig. 4: Foci are maintained for at least a 168 h under N starvation.

Representative PALM images of Hfq in *E. coli* cells under long-term N starvation. Images taken at N-24, N-48, N-72, N-96 and N-168.

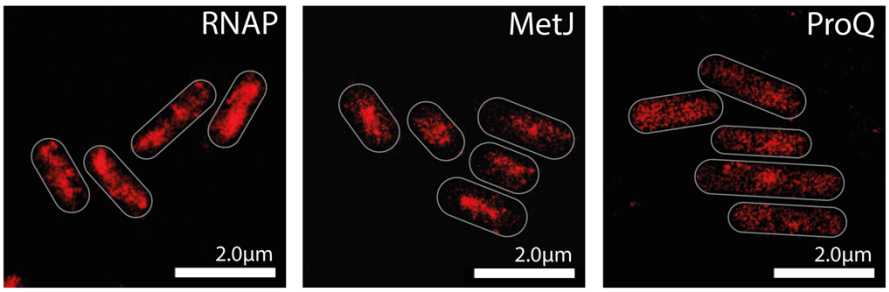

Supplementary Fig. 5: Foci formation is not a generic feature of proteins during N starvation.

Representative PALM images of RNA Polymerase (RNAP), MetJ and ProQ in *E. coli* cells at N-24.

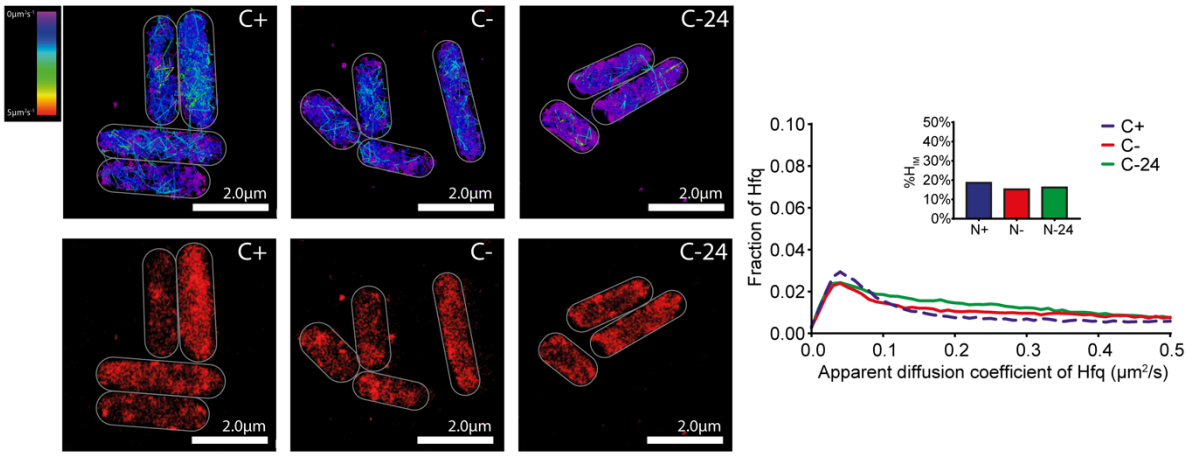

Supplementary Fig. 6: Hfq does not form foci in long-term C starved *E. coli* cells.

Representative PALM images and single molecule tracks of Hfq in *E. coli* cells during long-term C starvation. Images taken at C+, C- and C-24. The graph shows the distribution of apparent diffusion co-efficient (D^*) of Hfq molecules at the indicated time points and the corresponding $\%H_{IM}$ values are shown in the insert graph.

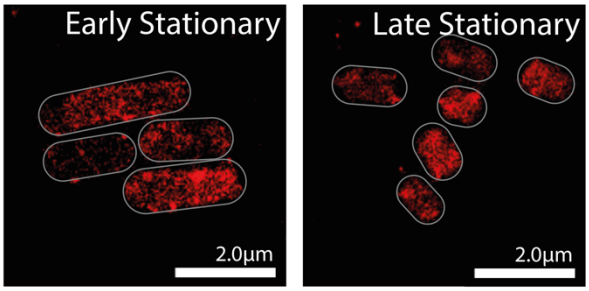

Supplementary Fig. 7: Hfq does not forms foci during stationary phase in lysogeny broth. Representative PALM images of Hfq in *E. coli* cells grown to early (1 h) and late (24 h) stationary phase in lysogeny broth.

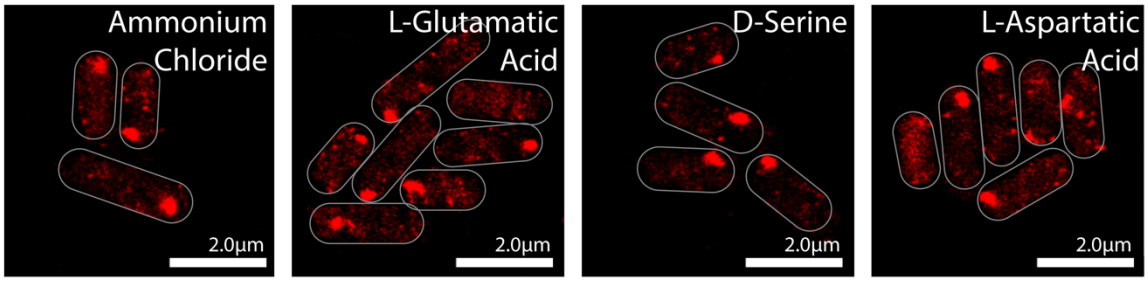

Supplementary Fig. 8: Hfq foci form when cells are initially grown in a range of alternate N sources.

Representative PALM images of Hfq in *E. coli* cells when 3mM of NH_4Cl, L-Glutamatic acid, D-Serine or L-Aspartatic acid was used as the sole N source. Cells for imaging were sampled at N-24, using growth in NH_4Cl as the reference.

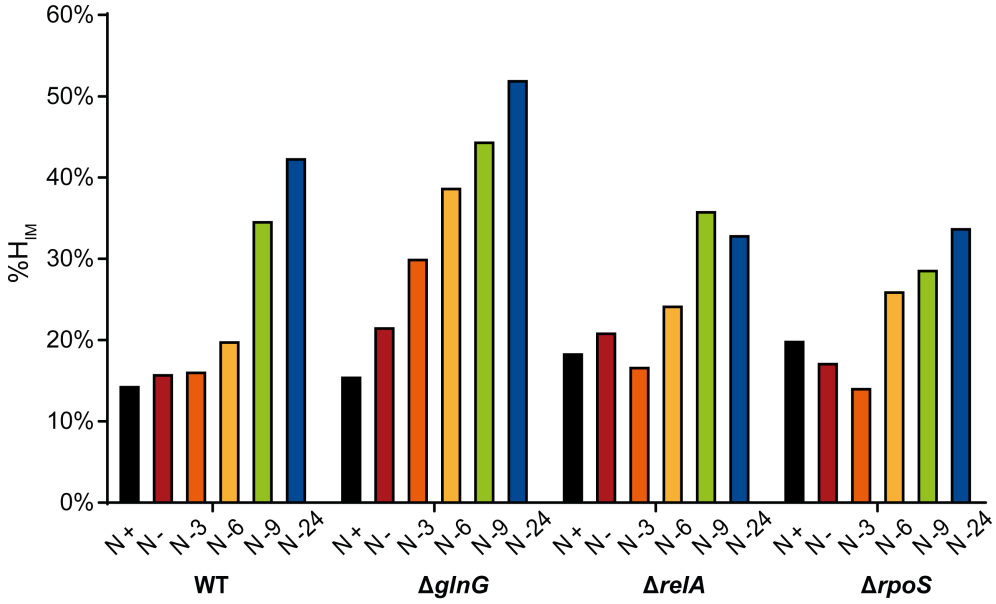

Supplementary Fig. 9: Hfq foci formation is a constituent process of the adaptive response to long-term N starvation in *E. coli.*

Graph showing $\%H_{IM}$ values of Hfq molecules in WT, Δ*glnG*, Δ*relA* and Δ*rpoS E. coli* cells at N+, N-, N-3, N-6, N-9 and N-24.

Supplementary Table 1: *E. coli* strains and plasmids used in this study.

Strains		
Name	Description	Source or Reference
Wild-type (BW25113)	*E. coli* K-12 (*araD-araB*)567 Δ(*rhaD-rhaB*) 568 Δ*lac*Z4787 (*::rrnB-3*) *hsdR*514 *rph*-1	E. coli Genetic Stock Center
Δ*hfq* (JW4130)	BW25113 Δ*hfq::kan*	E. coli Genetic Stock Center
Δ*rpoS* (JW5437)	BW25113 Δ*rpoS::kan*	E. coli Genetic Stock Center
Wild-type (MG1655)	*E. coli* K-12 *rph*-1	E. coli Genetic Stock Center
Hfq-FLAG	MG1655 *hfq*-3xFLAG	Provided by Prof. Jörg Vogel, University of Wurzburg
Hfq-PAmCherry	MG1655 *hfq-PAmCherry-kan*	This Study
MetJ-PAmCherry	MG1655 *metJ-PAmCherry-kan*	This Study
RpoC-PAmCherry (KF26)	MG1655 *rpoC-PAmCherry-kan*	[42]
Δ*ProQ*	MG1655 Δ*proQ::kan*	This Study
$Hfq_{\Delta 73\text{-}102}$ -PAmCherry	MG1655 $hfq_{\Delta 73\text{-}102}$*-PAmCherry-kan*	This Study
Δ*glnG* Hfq-PAmCherry	Hfq-PAmCherry Δ*glnG::kan*	This Study
Δ*relA* Hfq-PAmCherry	Hfq-PAmCherry Δ*relA::kan*	This Study
Δ*rpoS* Hfq-PAmCherry	Hfq-PAmCherry Δ*rpoS::kan*	This Study
Q8A Hfq-PAmCherry	Hfq-PAmCherry *hfq*-Q8A	This Study
D9A Hfq-PAmCherry	Hfq-PAmCherry *hfq*-D9A	This Study
R16A Hfq-PAmCherry	Hfq-PAmCherry *hfq*-R16A	This Study
R17A Hfq-PAmCherry	Hfq-PAmCherry *hfq*-R17A	This Study
Y25D Hfq-PAmCherry	Hfq-PAmCherry *hfq*-Y25D	This Study
K31A Hfq-PAmCherry	Hfq-PAmCherry *hfq*-K31A	This Study
Plasmids		
Name	Description	Source/Reference
pBAD24-*hfq*-FLAG	pBAD24 expressing *hfq*-3xFLAG under an arabinose inducible promoter	Provided by Prof. Jörg Vogel, University of Wurzburg
pBAD18	Empty pBAD18	[50]
pACYC-*proQ-PAmCherry*	Modified pACYC backbone (-TcR, +MCS) expressing *proQ-PAmCherry* under the native *proQ* promoter	This Study
pACYC-Hfq	Modified pACYC backbone containing Hfq under its native promoter	This Study

Supplementary Table 2: Primers used in this study.

Primers		
Name	5' to 3' Nucleotide sequence	Use
Hfq-PAmCherry 1	TTGCCCGAGGAGATTTGCAT	Fwd External Primer, for λ Red recombination
Hfq-PAmCherry 2	GAACCAGCAGCGGAGCCAGCCGATTCGGTTTCTTCGCTGTCCTGTT	Upstream of Hfq stop + Start PAmCherry-KanR, for λ Red recombination
Hfq-PAmCherry 3	AACTAAGGAGGATATTCATATGGGGTTTCGGGCTGTTTTTTTACACG	Downstream of Hfq stop + End PAmCherry-KanR, for λ Red recombination
Hfq-PAmCherry 4	GCACAAACGCTCCAGGTTAC	Rv External Primer, for λ Red recombination
Q8A Fw	CTAAGGGGCAATCTTTAGCAGATCCGTTCCTGAAC	Directed mutagenesis Hfq
Q8A Rv	GTTCAGGAACGGATCTGCTAAAGATTGCCCCTTAG	Directed mutagenesis Hfq
D9A Fw	GCAATCTTTACAAGCTCCGTTCCTGAACGC	Directed mutagenesis Hfq
D9A Rv	GCGTTCAGGAACGGAGCTTGTAAAGATTGC	Directed mutagenesis Hfq
R16A Fw	GTTCCTGAACGCACTGGCACGGGAACGTGTTCCAG	Directed mutagenesis Hfq
R16A Rv	CTGGAACACGTTCCCGTGCCAGTGCGTTCAGGAAC	Directed mutagenesis Hfq
R17A Fw	CCTGAACGCACTGCGTGCAGAACGTGTTCCAGTTTC	Directed mutagenesis Hfq
R17A Rv	GAAACTGGAACACGTTCTGCACGCAGTGCGTTCAGG	Directed mutagenesis Hfq
Y25D Fw	GAACGTGTTCCAGTTTCTATTGACTTGGTGAATGGTATTAAGCTG	Directed mutagenesis Hfq
Y25D Rv	CAGCTTAATACCATTCACCAAGTCAATAGAAACTGGAACACGTTC	Directed mutagenesis Hfq
K31A Fw	TTATTTGGTGAATGGTATTGCGCTGCAAGGGCAAATCGAG	Directed mutagenesis Hfq
K31A Rv	CTCGATTTGCCCTTGCAGCGCAATACCATTCACCAAATAA	Directed mutagenesis Hfq